ELSEVIER

Polymer 43 (2002) 1695–1699

polymer

www.elsevier.com/locate/polymer

Polymer Communication

Polymer nanocomposite coatings with non-linear elastic response

V.V. Tsukruk*, A. Sidorenko, H. Yang

Department of Materials Science and Engineering, Iowa State University, 3053 Gilman Hall, Ames, IA 50011, USA

Received 20 June 2001; received in revised form 25 October 2001; accepted 31 October 2001

Abstract

We fabricated polymer nanocomposite layered coatings with distinguished, non-linear nanomechanical behavior. The tri-layer film, with a total thickness of 20–30 nm, was composed of a hard topmost layer of a cross-linked poly(dimethacrylate), a compliant rubber interlayer, and a self-assembled monolayer chemically tethered to a silicon substrate. Nanometer scale deformation of this coating produced a non-linear elastic response with high initial resistance followed by more compliant behavior before higher resistance showed up again in highly compressed (about 60% of initial thickness) state. Deformation of the film was completely reversible due to the properties of the rubber interlayer and the grainy microstructure of the topmost layer. Such non-linear surface behavior is quite unique and brings a new prospective in the design of organized surfaces with tailored nanomechanical response.

Keywords: Multilayered coatings; Non-linear elasticity; Nanocomposite coatings

1. Introduction

Micro and nanomechanical surface properties reflect the microstructural organization of the topmost material layer. A vast majority of materials shows a relatively uniform micromechanical response at different levels of elastic deformation and indentation depth. This behavior is caused by similar microstructure of both the surface and internal bulk material. Two other scenarios, which are sometimes observed include higher initial surface stiffness (metals with oxide surface layers), and lower surface elastic modulus (polymeric materials with surface-segregated low molar weight fraction) [1–6]. In such cases, micromechanical response varies monotonically with indentation depth. The character of micromechanical response at very small deformations (nanometer-scale indentation depths) is especially critical for ultrathin compliant coatings of micromechanical devices. For such devices, the dynamic state of mating surfaces critically depends upon normal and shear stresses produced within a nanometer scale contact area [1,2,7,8].

Here, we report a new design; a compliant nanoscale coating with a total thickness below 30 nm, which demonstrates a *non-linear nanomechanical response*. The compression elastic modulus of this multilayered coating is a pre-determined and non-monotonic function of the external load and deformational level. The coating is composed of a hard, cross-linked polymethacrylate layer tethered to a compliant interlayer from a reinforced rubber phase that is grafted, in turn, to a epoxysilane self-assembled monolayer (SAM) chemically tethered to a silicon surface (Fig. 1).

2. Experimental

1,6-Hexanediol dimethacrylate and photoinitiator 4-(dimethylamino) benzophenone (PI) were purchased from Aldrich and used as received. Highly polished single-crystal silicon wafers of the {100} orientation (Semiconductor Processing Co.) were used as a substrate after cleaning with 'piranha' solution. (3-Glycidoxypropyl) trimethoxysilane was purchased from Gelest Inc. and was used to prepare epoxy-terminated SAM on the silicon surface [9,10]. The primary compliant layer was formed from the tri-block copolymer, poly[styrene-*b*-(ethylene-*co*-butylene)-*b*-styrene] (SEBS) (Kraton 1901, Shell), with styrene and maleic anhydride contents of 29 and 2 wt%, respectively, and molecular weight $M_n = 41,000$ g/mol. This layer was grafted to the epoxy-terminated SAM according to the procedure described in detail earlier [11–14]. The thickness of the grafted SEBS layer was 8.4 ± 0.4 nm. The solution of monomers was deposited directly onto the grafted SEBS layer, covered with a glass plate, and exposed to UV light to initialize photopolymerization. After polymerization, the samples were rinsed thoroughly with toluene

* Corresponding author. Tel.: +1-515-294-6904; fax: +1-515-294-5444.
E-mail address: vladimir@iastate.edu (V.V. Tsukruk).

0032-3861/02/$ - see front matter
PII: S0032-3861(01)00741-8

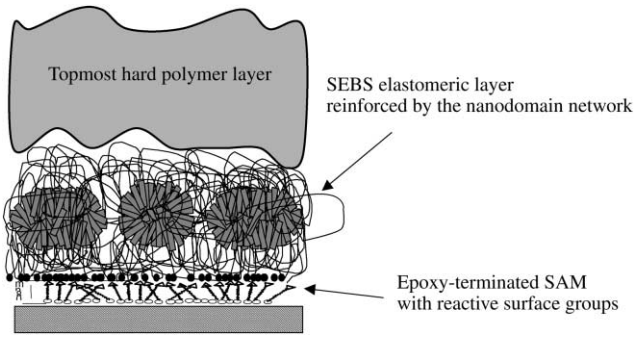

Fig. 1. Tri-layer nanocomposite coating with three molecular layers of different elastic properties (hard–compliant–hard) grafted to a silicon surface.

and treated in an ultrasonic bath to remove residual monomer and ungrafted polymer.

The thickness of the polymer layers was determined independently from ellipsometry measurements. Scanning probe microscopy (SPM) imaging was performed using tapping mode with a Dimension 3000 (Digital Instruments Inc.) microscope according to the usual procedure adapted in our lab [15–17]. Micromechanical measurements and surface micromapping were carried out in the contact mode according to the experimental procedure described earlier [18–20].

3. Results and discussion

The poly(1,6-hexanediol dimethacrylate) (PHDM) layers with the thickness in the range from 10 to 22 nm, formed on top of the pre-formed SEBS interlayer, showed continuous and uniform morphology over large surface areas with the microroughness in the range of 3–4 nm for the 1×1 μm area (Fig. 2). Nanograiny morphology of the topmost layer was clearly visible at higher magnifications (Fig. 2). Polymer grains observed at certain degrees of polymerization had sizes below 100 nm and were interconnected with each other to form a continuous layer. This microstructure was formed at intermediate stages of polymerization because of the microheterogeneous cross-linking reaction typical for these compounds [21,22]. Longer polymerization time leads to more uniform surface morphology with the grainy texture still clearly visible. The microstructure of the underlying SEBS interlayer was preserved under variable photopolymerization conditions as will be discussed in detail in a separate publication [25].

The hard PHDM layer is tethered to the compliant interlayer (as was verified with pull-off test) that is, in turn, grafted to epoxy-terminated SAM (Fig. 1). Such mutual tethering prevents delamination of dissimilar layers during large mechanical deformation of the tri-layer coating. On the other hand, preservation of the individual microstructure of different layers ensures their different micromechanical

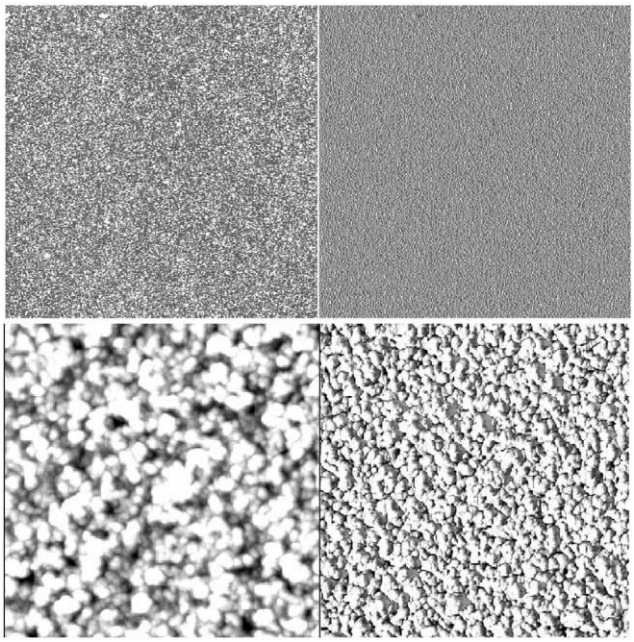

Fig. 2. SPM topographical (left) and phase (right) of the topmost layer surface: $5\ \mu m \times 5\ \mu m$ surface area showing uniform coverage with the topmost layer (top), $1\ \mu m \times 1\ \mu m$ area with higher resolution demonstrating grainy texture (bottom).

properties. These properties were measured for the independent reference samples as following. The PHDM layer was a hard plastic with the thickness in the range from 10 to 22 nm and the elastic modulus of about 2 GPa. The reinforced rubber interlayer was highly compliant with elastic modulus below 100 MPa [26]. The solid epoxysilane SAM had the thickness of 0.7–0.9 nm and estimated elastic modulus of about 1 GPa. Finally, the whole tri-layer was grafted to a solid substrate, the [100] silicon surface, with elastic modulus of 190 GPa [1].

Fig. 3 displays the surface morphology of the tri-layer film with an intentionally produced (with pull-off test) central hole. This hole penetrates the 14 nm topmost layer down to the rubber interlayer as can be seen from the cross-sectional analysis of the surface topography presented in Fig. 3(d). This type of location was used for measuring micromechanical surface properties. Micromapping of surface micromechanical response was performed with a pixel-by-pixel nanoindentation of the tri-layer coating similar to the procedure described earlier [20]. Indentation depth was kept within the range of 2–20 nm (very first 1–2 nm of indentation usually are masked by cantilever instability during jump-in contact [18]). These conditions for nanoprobing provided spatial resolution of 0.2 nm in the vertical direction and 10–50 nm within the x, y plane.

Surface distribution of adhesive forces and elastic response showed a clear correlation with surface topography. In that, highest adhesion and elastic modulus were observed within the hole (Fig. 3). Higher adhesion of the rubber interlayer is a result of its higher compliance, which

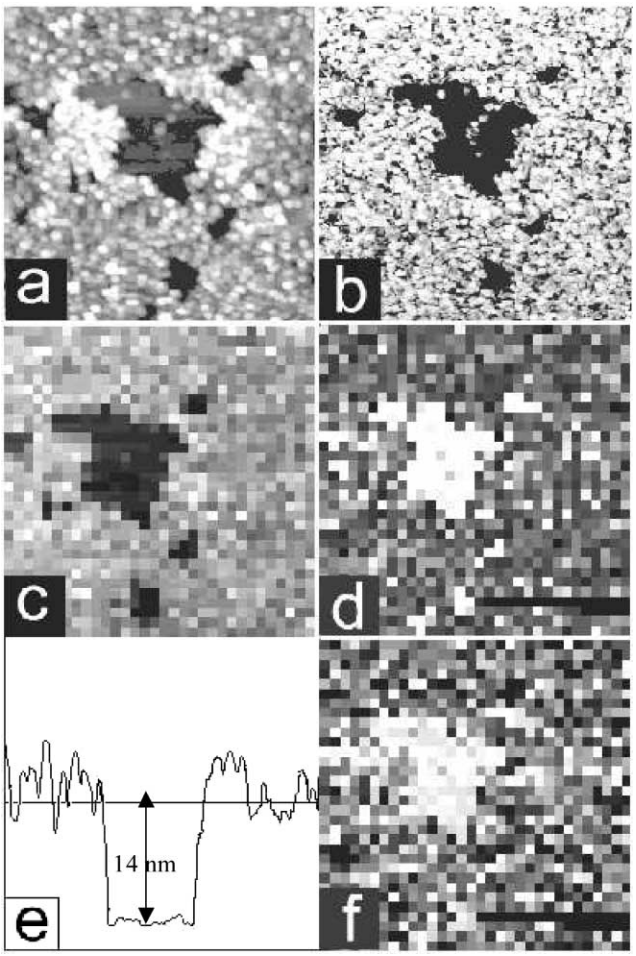

Fig. 3. SPM topographical (left) and phase (right) of the film surface with a central hole produced during pull-off test, 3 μm × 3 μm surface area with clearly visible grainy microstructure (a, b). Micromapping of surface properties of the film with 32 × 32 pixel resolution within the same surface area (c–f): topography (c), elastic modulus (d), and adhesive forces (f). Cross-section (e) of the center of the images shows the thickness of the topmost layer of 14 nm that corresponds to the value obtained from ellipsometry.

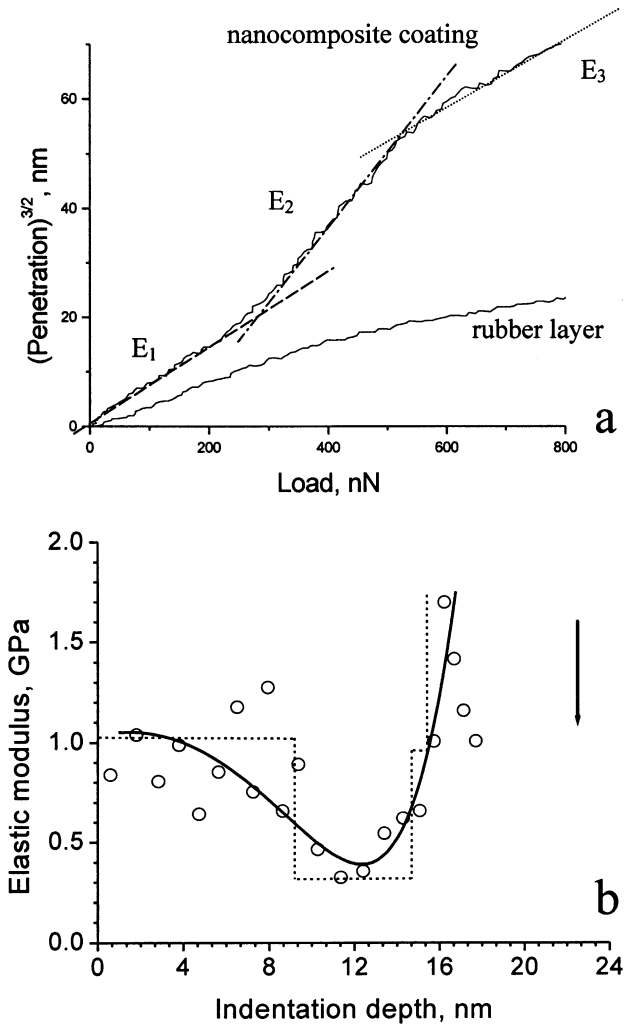

Fig. 4. (a) Penetration–loading curve converted from the original force–distance curve experimental data for the tri-layer coating in comparison with the rubber layer presented in Hertzian coordinates $d^{3/2}$ vs. load (for such a representation, slope of the linear fit directly gives elastic modulus) showing three load ranges with different elastic moduli. (b) Calculated depth profile of elastic modulus showing clearly three ranges with different levels of elastic responses. A box model (c, dots) shows expected idealized elastic response assuming the final compression of 60% for the whole tri-layer film. Arrow indicates the total thickness of the films. Solid line in Fig. 4(b) is a guide for an eye.

led to a larger contact area at a pull-off point [14]. Higher 'apparent' elastic modulus within the hole is caused by the underlying silicon substrate [26].

Penetration–load plots obtained from force–distance curves within the double-spring approach [18] clearly demonstrate non-linear nanomechanical response of the nanocomposite coatings with three load ranges having different slopes (Fig. 4(a)). Data are presented in the Hertzian coordinates, which should give a linear relationship if elastic modulus is constant [24]. Lower slope (stiffer response) is observed for very small deformations, right after the initial physical contact between the SPM probe and surface, and at very high deformations. Higher slope (more compliant response) is consistently recorded in the middle range of loads and indentations. A similar response for the rubber layer is located much lower due to its smaller thickness and deformational constraints imposed by the silicon substrate.

To quantify this behavior, we used analysis of elastic response in accordance with theories of elastic mechanical contact [23,24]. As was shown earlier, this technique is sensitive to nanoscale detail of the micromechanical behavior and can provide data about depth distribution of elastic modulus [20]. Application of the Hertzian model in this case can be considered only for a single probe displacement from point i to $i + 1$. For such a singe step, this model provides 'current' value of elastic modulus considered to be constant for the i stratum, E_i. However, for the evaluation of the next displacement, from $i + 1$ to $i + 2$, elastic modulus is considered to be a new unknown with its current new value, E_{i+1}, to be determined again with such an iterative procedure. The

model used in this approach is an expansion of the double-spring model introduced in our earlier papers [18,19], and can be called a double spring model with a variable spring constant. It is clear that this approach oversimplifies the actual situation representing media with gradient mechanical properties as a series of independent strata with different elastic moduli. The absolute values of elastic modulus obtained within this model should be considered cautiously as semi-quantitative (apparent moduli). Full scale analysis should include developments of data processing routines for more complicated gradient or multi-layered models, which is beyond the scope of current studies [6,27].

Depth profiling of elastic response of the fabricated tri-layer film obtained in the manner described above, indeed, confirmed the non-linear character of its micromechanical behavior (Fig. 4(b)). Initial, very small deformations within 2–6 nm were mediated by the topmost hard PHDM layer and showed the composite elastic modulus near 1 GPa. Upon further deformation, the rubber interlayer accepted the majority of the load, and this resulted in a decrease of the apparent value of elastic modulus down to 300–400 MPa. Finally, both compressed layers were squeezed and pushed against less compliant SAM and the silicon surface, which caused dramatic increase of the apparent elastic modulus (Fig. 4(b)). Total compression of the tri-layer film without visible plastic deformation can be as high as 14–16 nm, or about 60% of the initial thickness. The idealized distribution of the elastic properties along the surface normal for the tri-layer film, uniformly compressed by 60% can be represented by a box model (Fig. 4(b)). From comparison of experimental data and the model, we concluded that the actual nanomechanical response correlated fairly well with expected response of the tri-layer coating. Subsequent scanning of the probed surface area verified that film deformation was completely reversible. The shape of elastic response differed over various surface areas depending upon the exact location of the SPM tip end (on top of the grains or in-between). However, its non-linear character remained consistent over the significant portion of the surface area.

In conclusion, we fabricated nanocomposite layered molecular coatings with distinguished non-linear nanomechanical properties. The tri-layer film with the total thickness of 20–30 nm composed of the hard topmost layer, the reinforced rubber interlayer, and the SAM chemically grafted to the silicon substrate. Nanometer scale deformation of such nanocomposite films produced a non-linear elastic response with high initial elastic resistance followed by a more compliant range before high resistance showed up again in the highly compressed (60% of the initial thickness) state. Deformation of the film was completely reversible due to the exceptional elastic properties of the rubber interlayer and the grainy nanophase structure of the topmost layer. Such non-linear surface behavior is unique and brings a new prospective in design of organized surfaces with tailored nanomechanical behavior of complicated nature.

The design introduced here can be important for applications such as molecular coatings for microelectromechanical devices [1,2,7]. Indeed, low surface compliance at low deformations can be instrumental in keeping a minute contact area for solid surfaces with sub-micrometer radius of curvature under static regime. However, initial motion under an increasing normal load can result in larger elastic indentation as the load is transferred to the more compliant interlayer with much lower shear modulus. Unloading of the mating surfaces upon returning to rest conditions should restore the initial surface properties due to the reversible relaxation of the rubber interlayer. Our preliminary studies of microtribological properties of these coatings demonstrated that their wear resistance is significantly (several times) higher than wear resistance of classic boundary lubricant, alkylsilane SAMs [25].

Acknowledgements

This work is supported by The US National Science Foundation, CMS-9996445 and 0099868 Grants. The authors thank Drs V.V. Gorbunov and I. Luzinov for numerous helpful discussions and D. Julthongpiput for technical assistance.

References

[1] Bhushan B, editor. Tribology issues and opportunities in MEMS. Dordrecht: Kluwer, 1998.
[2] Bhushan B, editor. Micro/Nanotribology and its applications. Dordrecht: Kluwer, 1997.
[3] Burnham NA, Dominguez DD, Mowery RL, Colton RJ. Phys Rev Lett 1990;64:1931.
[4] Briscoe BJ, Evans DC. Proc R Soc A 1981;380:389.
[5] Makushkin AP. Friction Wear 1990;11:423.
[6] Giannakopoulos AE, Suresh S. Int J Solids Struct 1997;34:2393.
[7] Tsukruk VV. Adv Mater 2001;13:95.
[8] Tsukruk VV, Wahl K, editors. Microstructure and microtribology of polymer surfaces. ACS Symposium Series, vol. 741. 2000.
[9] Tsukruk VV, Luzinov I, Julthongpiput D. Langmuir 1999;15:3029.
[10] Luzinov I, Julthongpiput D, Liebmann-Vinson A, Cregger T, Foster MD, Tsukruk VV. Langmuir 2000;16:504.
[11] Tsukruk VV. Tribol Lett 2001;10:127.
[12] Luzinov I, Julthongpiput D, Tsukruk VV. Polymer 2001;42:2267.
[13] Luzinov I, Julthongpiput D, Tsukruk VV. Macromolecules 2000;33:7629.
[14] Luzinov I, Julthongpiput D, Gorbunov VV, Tsukruk VV. Tribol Int 2001;35:335.
[15] Sarid D. Scanning force microscopy. New York: Oxford University Press, 1991.
[16] Tsukruk VV. Rubber Chem Technol 1997;70:430.
[17] Tsukruk VV, Reneker DH. Polymer 1995;36:1791.
[18] Chizhik SA, Huang Z, Gorbunov VV, Myshkin NK, Tsukruk VV. Langmuir 1998;14:2606.
[19] Tsukruk VV, Huang Z, Chizhik SA, Gorbunov VV. J Mater Sci 1998;33:4905.
[20] Tsukruk VV, Huang Z. Polymer 2000;41:5541.

[21] Kurdikar DL, Peppas NA. Polymer 1994;35:1004.
[22] Medvedevskikh JG, Zagladko EA, Turovski AA, Zaikov GE. Int J Polym Mater 1999;1:43.
[23] Johnson KL. In: Tsukruk VV, Wahl K, editors. Microstructure and microtribology of polymer surfaces, ACS Symposium Series, vol. 741. 2000. p. 24.
[24] Johnson KL, Kendall K, Roberts A. Proc R Soc 1971;324:301.
[25] Sidorenko A, Ahn Hyo-Sok, Kim Doo-In, Yang H, Tsukruk VV. Wear. Submitted for publication.
[26] Tsukruk VV, Sidorenko A, Gorbunov VV, Chizhik SA. Langmuir. 2001;17:6715.
[27] Stone DC. J Mater Res 1998;13:3207.